The EMBO Journal (2004) 23, 930–938 | © 2004 European Molecular Biology Organization | All Rights Reserved 0261-4189/04
www.embojournal.org

THE EMBO JOURNAL

Formation, maintenance and consequences of the imprint at the mating-type locus in fission yeast

Atanas Kaykov, Allyson M Holmes and Benoit Arcangioli*

Unité de Dynamique du Génome, URA 1644 Département de la Structure et Dynamique des Génomes, Institut Pasteur, Paris, France

Mating-type switching in the fission yeast *Schizosaccharomyces pombe* is initiated by a strand-specific imprint located at the mating-type (*mat1*) locus. We show that the imprint corresponds to a single-strand DNA break (SSB), which is site- but not sequence-specific. We identified three novel *cis*-acting elements, involved in the formation and stability of the SSB. One of these elements is essential for a replication fork pause next to *mat1* and interacts *in vivo* with the Swi1 protein. Another element is essential for maintaining the SSB during cell cycle progression. These results suggest that the DNA break appears during the S-phase and is actively protected against repair. Consequently, during the following round of replication, a polar double-strand break is formed. We show that when the replication fork encounters the SSB, the leading-strand DNA polymerase is able to synthesize DNA to the edge of the SSB, creating a blunt-ended recombination intermediate.

The EMBO Journal (2004) **23,** 930–938. doi:10.1038/sj.emboj.7600099; Published online 12 February 2004
Subject Categories: genome stability & dynamics
Keywords: fission yeast; imprinting; mating type; recombination; replication

Introduction

In the fission yeast *Schizosaccharomyces pombe*, a stable single-strand DNA lesion triggers programmed gene conversion at the mating-type locus. This process restricts mating-type interconversion to one of the two sister chromatids during DNA replication. Following chromosome segregation at mitosis, the sister cells express two different and complementary mating-type alleles (Arcangioli and Thon, 2003). Extensive pedigree analysis at the single-cell level demonstrated that two consecutive divisions are required to produce one switched cell among four related cousins. Furthermore, the sister of the switched cell is competent for switching during the next division, forming a chain of recurrent switching (Miyata and Miyata, 1981; Egel and Eie, 1987; Klar, 1987, 1990). It was proposed that an imprinting event segregates with a specific strand of DNA at the mating-type locus (*mat1*) (Klar, 1987). The mating type of the cell is determined by the allele present at the *mat1* locus on the right arm of chromosome II: *mat1*P in P cells and *mat1*M in M cells (Beach *et al*, 1982). The *mat1* allele can be replaced efficiently by genetic information contained in one of the two silent donor cassettes *mat2*P and *mat3*M (Beach, 1983; Kelly *et al*, 1988). A noticeable feature of the mating-type loci is that they are flanked by homologous sequences (Figure 1A). The H1 homology box (59 bp) is located on the centromere-distal side of the cassettes and the H2 homology box (135 bp) on the centromere-proximal side (Kelly *et al*, 1988). Both sequences are thought to be essential for base pairing during the initiation and resolution steps of the gene conversion process required for mating-type switching.

Recent molecular studies suggest that the imprint at *mat1* is either a single-strand DNA break (Arcangioli, 1998) or an alkali-labile DNA modification (Dalgaard and Klar, 1999). The discovery of this novel type of single-strand DNA lesion (called SSB) has triggered new investigations of the mating-type interconversion process. The SSB was mapped to the upper strand at the junction of the *mat1* allele and the H1 homology box. This SSB fulfills all of the imprinting criteria described previously for mating-type switching (Crouse, 1960; Klar, 1987). Interestingly, the position of the break at *mat1* differs by three nucleotides between the *mat1*P and *mat1*M alleles (Nielsen and Egel, 1989; Arcangioli, 1998). The enzyme or process involved in the SSB formation at *mat1* is unknown. The SSB is stable throughout the entire length of the cell cycle and is transiently converted to a polar double-strand break (DSB) during the S-phase. The DSB appears on the distal side of *mat1*, indicating that the replication fork is approaching *mat1* from the H1 side (Arcangioli, 1998). Consequently, it was proposed that the leading-strand replication complex is stalled at or near the SSB. The broken chromatid can be healed by a gene-conversion event, initiated at the H1 homology sequence also present at the opposite donor loci. Once DNA repair synthesis starts, it proceeds into the silent locus ending after the H2 homology region (Arcangioli and de Lahondes, 2000). Several recent experiments indicate that the polarity of replication at *mat1* is achieved by a replication termination site (*RTS1*) located about 700 bp centromere-proximal to the H2 box, thus forcing the locus to be replicated from the H1 side, a necessary condition for SSB formation. Another element called *MPS1* (for *mat1* pause site I) was also described around the H1 box as important in SSB pathway formation (Dalgaard and Klar, 1999, 2000). We showed that the SSB is reformed at every generation on the newly synthesized upper DNA strand (Arcangioli, 2000). Taken together, these experiments demonstrate that following DNA replication, the SSB is found on the upper, neo-synthesized lagging strand.

Functional studies of the region centromere-distal to *mat1* revealed the presence of two *cis*-acting elements, SAS1 and SAS2 (for switching-activating sites), located 140 and 60 bp from the break at *mat1* (Arcangioli and Klar, 1991). The

*Corresponding author. Unité de Dynamique du Génome, URA 1644 du CNRS, Département de la Structure et Dynamique des Génomes, Institut Pasteur, Jacques Monod Building, 25 rue du Dr Roux, F-75724 Paris Cedex 15, France. Tel.: +33 1 4568 8454; Fax: +33 1 4568 8960; E-mail: barcan@pasteur.fr

Received: 23 September 2003; accepted: 15 December 2003; Published online: 12 February 2004

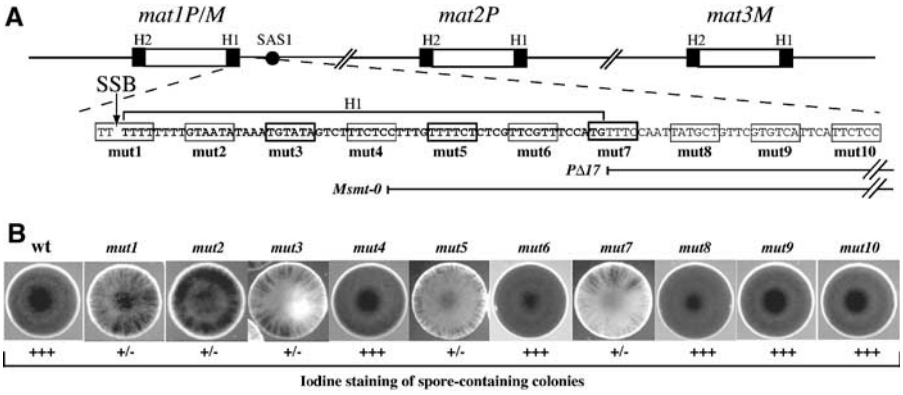

Figure 1 Structure of the mating-type region and phenotypes of the *cis*-acting mutations. (**A**) Schematic representation of the mating-type loci on the right arm of chromosome II. The black boxes indicate the H1 and H2 homology sequences and the SAS1 element is shown as a black circle. The H1 sequence is in bold and an arrow indicates the position of the SSB. The positions of the *Pst*I (CTGCAG) substitutions are indicated by rectangles and numbered (mut1–mut10) and the *Msmt-0* and *PΔ17* deletions are shown. (**B**) The switching efficiencies for the mutant strains (*mut1* to *mut10*) were analyzed by exposing the colonies to iodine vapors. The *Pst*I substitutions at positions 1, 2, 3, 5 and 7 reduce (+/−) the switching efficiencies.

switching-activating protein Sap1 interacts with SAS1 (Arcangioli *et al*, 1994) and is essential for growth, independently of mating-type switching, and participates in chromosome morphogenesis (de Lahondès *et al*, 2003). Individual deletions of SAS1 or SAS2 reduced the level of the break and double deletions abolished break formation. Similar deletions in M or P strains have been named *Msmt*-0 or *PΔ17*, respectively (see Figure 1; Arcangioli and Klar, 1991; Styrkarsdottir *et al*, 1993). Three *trans*-acting gene products (Swi1p, Swi3p and Swi7p) were identified as necessary for the initial formation of the lesion, since their mutations cause a reduced steady-state level of the SSB. Swi1 (Egel *et al*, 1984) has sequence identity in many species and was named topoisomerase 1-associated factor 1 (Tof1) in *Saccharomyces cerevisiae*, where it was shown to regulate DNA damage responses during the S-phase (Park and Sternglanz, 1999; Dalgaard and Klar, 2000; Foss, 2001). *swi7* encodes the catalytic subunit of the DNA polymerase α (Singh and Klar, 1993). The replication-pausing activities of both *RTS1* and *MPS1* are strongly reduced in *swi1* or *swi3* mutants, whereas the activity of at least *MPS1* is not affected in *swi7* or *Msmt*-0 mutants. It was therefore proposed that *swi1* and *swi3* act upstream of *swi7* and the *cis*-acing SAS1 and SAS2 elements in SSB pathway formation (Dalgaard and Klar, 2000, 2001).

To advance our understanding of the process of SSB formation and stability, we undertook a functional analysis of the DNA sequence at the SSB site and within its vicinity. To preserve the distances between already known and novel elements, we introduced substitution mutations. Several new sequences located within the H1 homology box were characterized as essential for the SSB steady-state level, and consequently for mating-type switching. Using several molecular approaches (two-dimensional (2D) gel electrophoresis, genomic sequencing and chromatin immunoprecipitation), we were able to ascribe specific activities to these novel elements and propose a model for SSB formation and maintenance. Significantly, we found that during DNA replication, the leading-strand DNA polymerase synthesizes DNA until the last 5′ nucleotide of the broken DNA, forming a blunt-ended recombination intermediate.

Results

Identification of novel cis-acting elements necessary for efficient mating-type switching

Systematic linker-scanning mutagenesis was performed within the H1 sequence distal to *mat1*. Each mutation consists of a 6 bp *Pst*I substitution located within every 10 bp, starting from the SSB and extending 100 bp from the break site, and are named *mut1–mut10* (Figure 1A). As the mutated DNA fragments contain the *mat1*P allele, following homologous recombination, each mutant initially expresses the P mating type. The mutants were first analyzed by the iodine-staining assay, an indirect measure of the mating-type switching efficiency. The starch reaction with iodine vapors stains spore-containing colonies black, whereas slow-switching mutants exhibit streaky iodine-staining patterns and colonies unable to switch the mating type appear yellowish. The position of the mutations (*mut1–mut10*) and their effects on iodine staining are shown in Figures 1A and B. None of the mutations completely abolished mating-type switching. Five mutations (*mut1*, *mut2*, *mut3*, *mut5* and *mut7*) exhibit variable streaky staining, indicative of reduced switching efficiencies, whereas the five other mutations appear to have no effect (*mut4*, *mut6*, *mut8*, *mut9* and *mut10*). The *mut7* mutation pinpoints the *cis*-acting SAS2 element, grossly mapped by deletional analysis (Arcangioli and Klar, 1991). Interestingly, the first three mutations (*mut1*, *mut2* and *mut3*), upon re-streaking, produce a noticeable proportion of black colonies by iodine staining. As this staining was stable and similar to wild-type levels, we hypothesized that these were spontaneous revertants of the mutation. To quantify the rate of reversion, we counted the percentage of colonies that were half black and half streaky. As shown in Figure 2A, the efficiency of reversion decreased as a function of distance from the DNA lesion (*mut1* > *mut2* > *mut3*). The other mutations were also tested and showed no detectable reversion of the *Pst*I site (data not shown). To demonstrate that reversion indeed occurred, we prepared DNA from two independent clones from each mutant and amplified the DNA sequence flanking the SSB, using primers specific for the P or M alleles at *mat1* (Figure 2B). Amplified DNA fragments were

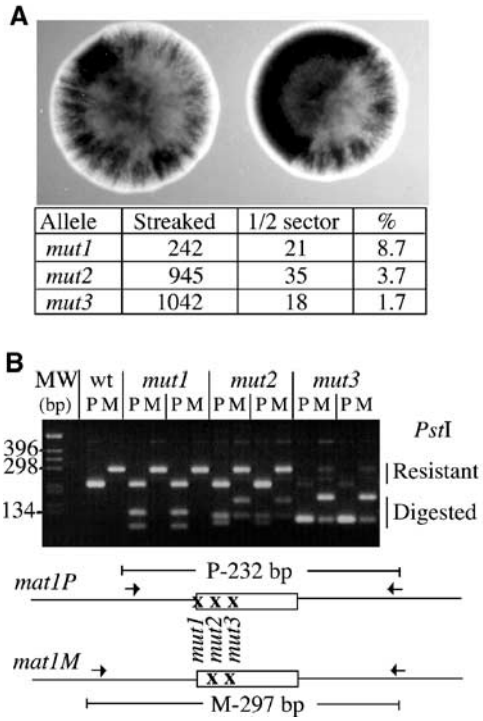

Allele	Streaked	1/2 sector	%
mut1	242	21	8.7
mut2	945	35	3.7
mut3	1042	18	1.7

Figure 2 Reversion of the *mut1*, *mut2* and *mut3* substitutions. (**A**) Reversion rates for strains (*mut1*, *mut2* and *mut3*) per cell division were calculated from the number of half-black sectors per streaky colonies. (**B**) DNA from two independent streaky colonies in each strain was isolated, and amplified with two different sets of primers specific for *mat1*P (P) or *mat1*M (M), and analyzed for the presence of the *Pst*I site. The *mat1*M and *mat1*P PCR products from wild-type DNA are resistant to *Pst*I. Upon growth, the *mut1* mutant gives rise to a *mat1*M allele, completely resistant to *Pst*I digestion. The *mut2* and *mut3* give rise to a mixed population of resistant and digested DNA for both P and M alleles. The differential migration of the *Pst*I-digested PCR products is due to the position of the *Pst*I sites.

assayed for the presence of the *Pst*I mutation by enzymatic digestion. From each of the three mutants, we isolated DNA resistant to *Pst*I digestion, which correlated with the rate of reversion obtained by iodine staining (*mut1* > *mut2* > *mut3*), and DNA sequences were identical to the wild type. Interestingly, *mut1* never gave rise to *Pst*I at the M allele (see Discussion).

Effects of the mutations on the SSB steady-state levels and position

As the reduced *mat1* switching efficiency can be due to reduced SSB formation, we analyzed the level of the break for each mutant strain. Genomic DNA from each strain was prepared using the traditional DNA extraction procedure, which converts the SSB to a DSB by shearing the fragile site (Arcangioli, 1998). We observed the three *mat1 Hind*III DNA fragments of 12.6 kbp, together with the two sheared products *mat1*-distal and *mat1*-proximal of 7.2 and 5.4 kbp, respectively (Figure 3A). Strains *mut3*, *mut5* and *mut7* exhibit reduced levels of the *mat1* cut fragments, indicating reduced steady-state levels of the break, consistent with reduced switching efficiencies. However, *mut1* and *mut2* mutations, which exhibit a mild reduction of the switching phenotype, showed wild-type levels of the break. Importantly, when the genomic DNA was subsequently digested with *Pst*I, we never observed transfer of the mutated sequence into the silent *mat2*P and *mat3*M loci (data not shown). The phenotypes observed (iodine staining and break level) were not due to the insertion of the *LEU2* gene, since several mutations were introduced without *LEU2* to confirm the mutant phenotypes (Arcangioli and Klar (1991) and data not shown). We used the genomic sequencing methodology to map the position of the SSB in each mutant. Genomic DNA was prepared from wild-type and mutant (*mut3*, *mut5* and *mut7*) strains using low-melting agarose plugs, which protect the fragile site from shearing (Arcangioli, 1998). For each mutant, the SSB is present on the upper strand, and in the same position as the wild-type break, but at reduced levels (Figure 3B). As previously shown, two *mat1*-distal upper DNA strands, of 233 and 236 nucleotides, were observed, corresponding to the SSB at *mat1*M and *mat1*P, respectively (Nielsen and Egel, 1989; Arcangioli, 1998). To avoid the high rate of reversion observed in *mut1*, we used a stable *mat1*M strain with a deletion of the *mat2*P and *mat3*M silent cassettes (strain SP714). This strain is viable and contains wild-type levels of the SSB (Klar and Miglio, 1986). The same *Pst*I mutation, as previously used for the P allele (*mut1*), was introduced into the M allele, in this stable donorless background (named *mut1-3*). Figure 3C shows that *mut1-3* exhibits a SSB on the upper strand, at the same position and level as compared to the parental SP714 strain. From this result, we conclude that the SSB is site-specific and sequence independent.

mut3 reduced Swi1p interaction at mat1 and the replication pause at MPS1

The replication fork pause *MPS1* appears to be a prerequisite for SSB formation and was reported to be fully active in the *Msmt*-0 mutant strain, containing a 262 bp deletion, that removes all of the *cis*-acting elements starting from the mut4 position and extends beyond SAS1 (Figure 1A). We investigated whether the *mut3* mutation affects the *MPS1* pause site by 2D gel electrophoresis (Brewer and Fangman, 1988). *mut3* exhibits a reduced pausing efficiency compared to the wild-type and the two other mutant strains *mut5* and *mut7* (Figure 4A). As *swi1* was previously shown to be important for *MPS1* function, we tested whether Swi1p interacts *in vivo* with this DNA element by chromatin immunoprecipitation (ChrIP). We constructed a strain containing an HA tag of Swi1 (AHR1, see Materials and methods). This strain, which exhibits wild-type levels of mating-type switching, SSB formation and *MPS1* activity (data not shown), was combined with *mut3*. Primer pairs flanking *mat1* were used for quantitative real-time PCR (Figure 4B) and semiquantitative PCR analyzed by agarose gel electrophoresis (data not shown) of DNA prepared from HA-immunoprecipitated material. The H1 sequence containing the *MPS1* element was strongly associated with Swi1 and this interaction was almost abolished in the *mut3*-containing strain (Figure 4B). Collectively, these data indicate that Swi1 interacts physically (directly or indirectly) with the sequence mutated at mut3 and that this interaction is required for DNA-replication pausing. A weaker Swi1 interaction was observed with the other side of *mat1*, containing the *RTS1* element in the wild-type background. However, the strain containing the *mut3* mutation, about 2 kbp away from *RTS1*, enhances the Swi1 interaction with *RTS1* in a

reproducible manner (Figure 4B and Materials and methods). This result suggests that Swi1 interacts with these two replication fork pause elements in a mutually exclusive manner.

Mut7 is essential to maintain the SSB during cell cycle progression

The high level and stability of the SSB suggests that the break is actively protected against repair during cell cycle progression and that its recombinational repair occurs within the same phase as its formation, namely the S-phase (Arcangioli 1998). To elucidate whether *mut3*, *mut5* and *mut7* substitutions affect the formation or maintenance of the SSB, we followed the level of the break during cell cycle progression. Small G2 cells were enriched from an asynchronous cell population, by lactose gradient centrifugation, and transferred to fresh media allowing cells to continue cycling in a synchronized fashion (Fantes and Nurse, 1978). Cell samples from the synchronized population were taken at 20 min intervals, and genomic DNA was prepared and analyzed by genomic sequencing. Figure 5A compares SSB levels among the wild-type and mutant strains during cell cycle progression. Like wild type, *mut3* exhibits constant levels of the SSB in all phases of the cell cycle, albeit with lower levels (Figure 5C). We obtained a similar result with a *swi1*-deleted strain (data not shown). In contrast, *mut7* shows variable levels of the SSB, which peaked at the 100 min time point and then diminished. This peak overlaps with the first replication period (S1), as measured by septation (Figures 5B and C). A second increase of the SSB was observed at the beginning of the second septation peak (200 min, at S2). A modest increase of the SSB level was also observed for *mut5* during the S-phase. A block and release experiment using hydroxyurea (HU), an inhibitor of ribonucleotide reductase, gives similar results (data not shown). These data indicate that the *mut7* mutation reveals an important *cis*-acting element (SAS2) necessary for maintaining the SSB during cell cycle progression, and strongly support the hypothesis that the SSB is formed during DNA replication.

Leading-strand polymerase synthesizes DNA to the edge of the SSB 5′ end

Maintaining the SSB at *mat1* is thought to be necessary for DSB formation during the next round of replication. However, the molecular nature of the broken-end intermediate depends on the ability of the leading-strand machinery to synthesize DNA to the 5′ edge of the DNA template. To enrich for replication intermediates, we used a strain containing the *cdc25-22* conditional mutant allele to synchronize the cell population. To reduce rapid disappearance of the 3′ end of the leading strand during gene conversion, the strain used was also donorless and *mat1*M stable. Cell samples from the synchronized population were taken at various intervals and genomic DNA was analyzed by genomic sequencing to

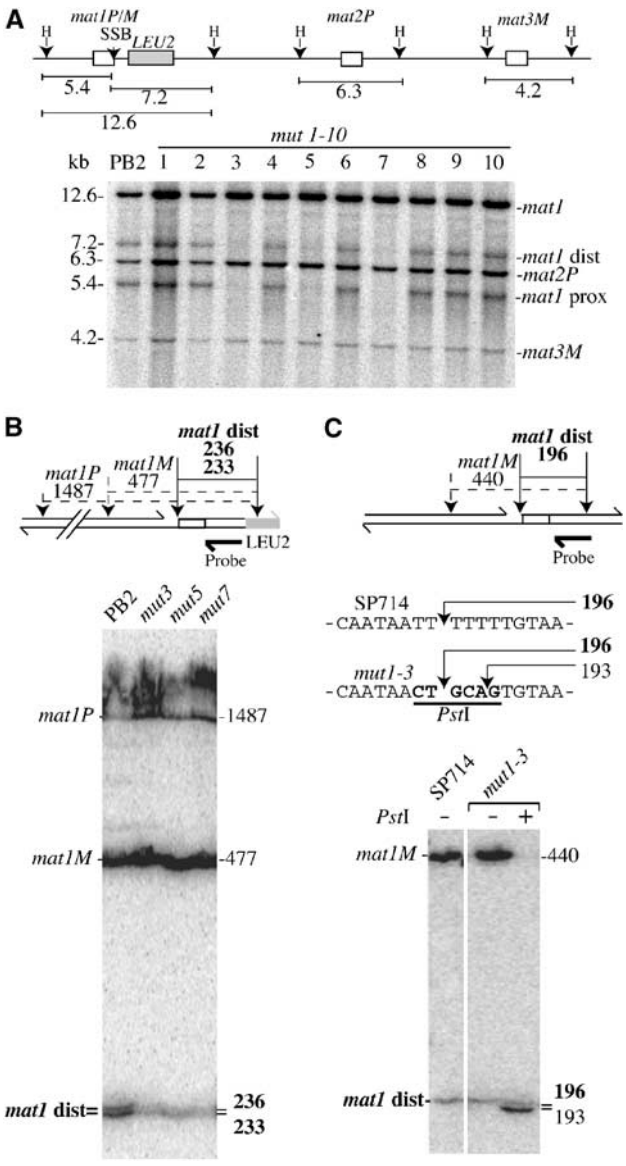

Figure 3 Level and position of the SSB in mutant strains. (**A**) Upper panel: Schematic representation of the mating-type region and size (in kbp) of the *Hind*III (H) DNA fragments. Genomic DNA from the wild-type (PB2) and each mutant strain (*mut1* to *mut10*) was prepared by the classical method, digested by *Hind*III and analyzed by Southern blot (lower panel). The probe used is a *mat1*P *Hind*III radiolabeled fragment. The SSB present in 20–30% of *mat1* molecules is transformed to a DSB during DNA purification. Therefore, the 12.6 kbp *mat1* fragment is broken into two subfragments (*mat1*-proximal, 5.4 kbp, and *mat1*-distal, 7.2 kbp). The probe also recognizes the *mat2*P (6.3 kbp) and *mat3*M (4.2 kbp) *Hind*III DNA fragments. (**B**) Upper panel: Positions and distances for the SSB (arrow) and the *Ssp*I restriction site polymorphisms (dotted arrows) in the *mat1*P and M loci. Note the position of the *LEU2* gene, which displaces the *Ssp*I site by 37 nucleotides. The probe used is a *mat1*-distal single-stranded radiolabeled fragment. The sizes and names of the DNA fragments are shown. Lower panel: Genomic sequencing analysis of the SSB in wild-type (PB2), *mut3*, *mut5* and *mut7* strains. The sizes and names of the labeled DNA fragments are indicated. (**C**) Position of the SSB in the stable *mat1*M donorless strains, SP714 and *mut1-3* (absence of *LEU2*). Upper panel: Positions and distances between the SSB (arrow) and the *Ssp*I sites (dotted arrows), located on both sides of the SSB. Sequences of the upper strand containing the SSB in the wild-type strain (SP714), and in the mutant strain *mut1-3*, containing the *Pst*I substitution (in bold), are indicated. Lower panel: Genomic DNA was prepared, digested with *Ssp*I and analyzed as above, with the sizes and names of the DNA fragments indicated. Upon *Pst*I digestion of the mutant DNA, the *mat1*M DNA fragment (440 nucleotides) was cleaved, liberating a 193 DNA fragment (no SSB and cut by *Pst*I), which migrates just below the wild-type 196 *mat1*-distal fragment (with the SSB and not cut by *Pst*I).

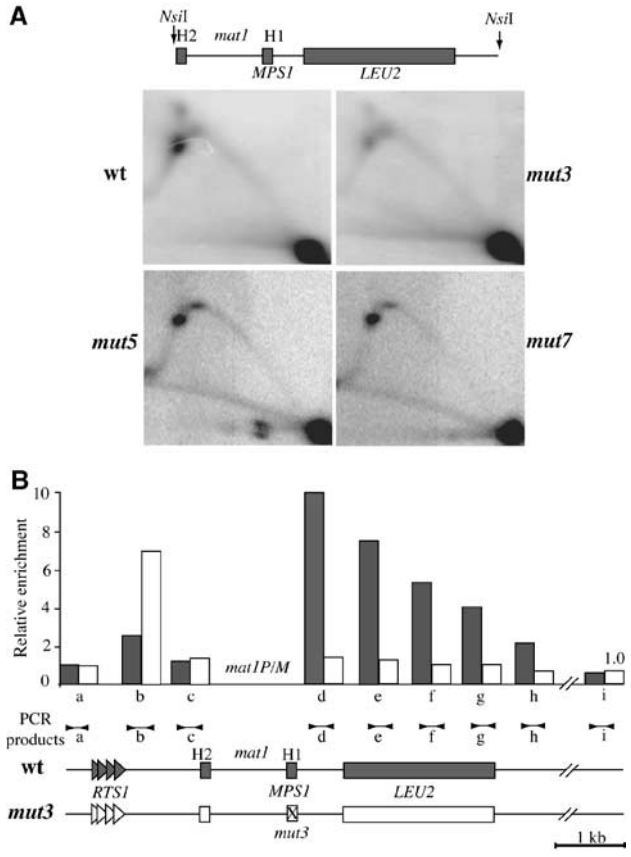

Figure 4 *mut3* strongly reduces *MPS1* activity and Swi1 interaction. (**A**) Analysis of replication intermediates in the wild-type, *mut3*, *mut5* and *mut7* strains by 2D gel electrophoresis. Schematic representation of the *mat1-Nsi*I restriction fragment. The quantification of the hybridization signals indicates that the *MPS1* spot is 10-fold lower for *mut3* (data not shown). (**B**) Chromatin immunoprecipitation analysis of Swi1p with the flanking *mat1* sequences. The lower panel shows the wild-type (AHR1) and *mut3*-containing strain (AHR2) in gray and white, respectively. The positions of *RTS1* and *MPS1* are indicated on both sides of *mat1*. Note that *mat1* was not analyzed since the same sequences are present at the two donor loci. Genomic DNA from wt (AHR1) and *mut3* (AHR2) strains was isolated from crude extracts and the anti-HA (Swi1) immunoprecipitated chromatin was assayed by quantitative PCR (Materials and methods). Each sample was assayed in triplicate, giving a standard deviation between 5 and 10% for the quantitation of the DNA sample. The positions of PCR products (a–i) are shown above the schematic representation of the *mat1* region. Following quantification, the relative enrichment for each PCR product was plotted, with the highest enrichment set at 10. The gray and white bars in the histogram indicate wt and *mut3*, respectively.

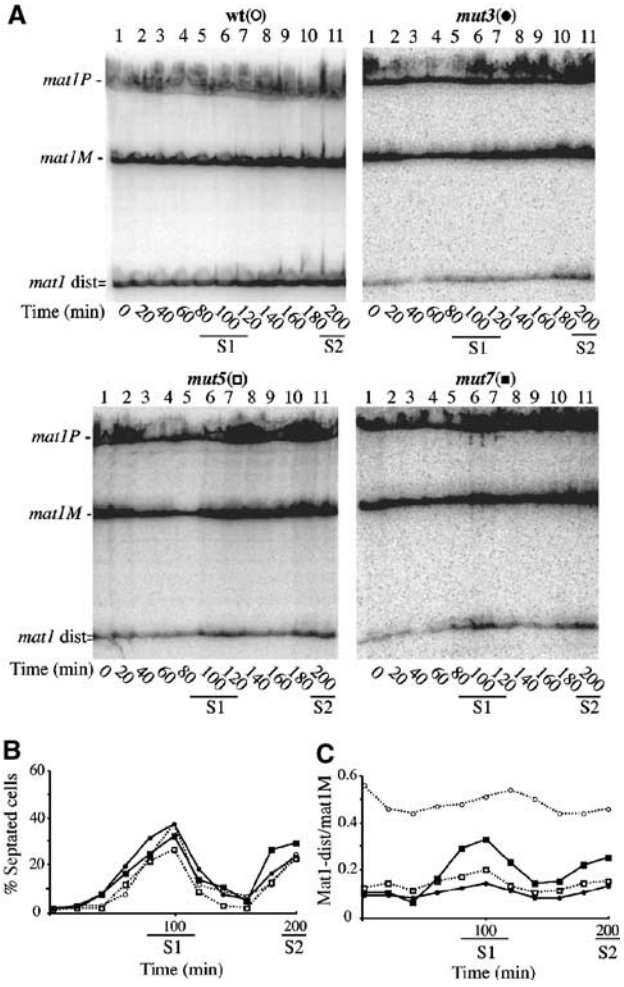

Figure 5 Stability of the SSB during cell cycle progression. Wild-type (○), *mut3* (●), *mut5* (□) and *mut7* (■) strains were synchronized by lactose gradients (enriching for small G2 cells) and samples from each culture were taken every 20 min. (**A**) Purified DNA was analyzed by genomic sequencing as in Figure 3B. (**B**) Cell cycle progression for each culture was followed by measuring the proportion of septated cells (as well as cell density, not shown) as a function of time for almost two generations (same strain symbols as used in (A)). Septum formation coincides with DNA replication period (indicated by S1 and S2) in *S. pombe*. (**C**) The intensity of the *mat1*M and *mat1*-distal bands was quantified using a PhosphoImager and the relative intensity of *mat1*-distal/*mat1*M, for each time point, was plotted (same strain symbols as used in (A)). The *mat1*-distal DNA fragment varied slightly during cell cycle progression for the wild-type, *mut3* and *mut5* strains, but peaked for *mut7* around the 100 and 200 min time points (same symbols). These results are representative of three independent experiments.

map the position of the 3′ end of the leading strand stalled at *mat1* (Figure 6A). Figure 6B shows the position and kinetics of the appearance and disappearance of a novel band overlapping the S-phase, peaking at the 70–90 min time points. Another band was present in all lanes and corresponds to the upper strand containing the SSB (data not shown). To estimate the size of the transitory band, we used the presence of the *Pst*I sites in the *mut1-3* and *mut1-4* strains (*mat1*M, donorless background) as size markers (Figure 6F, right panel). Upon *Pst*I digestion, *mut1-4* and *mut1-3* produce lower-strand DNA fragments, of wild-type sequence, with a one-nucleotide resolution between them (196 and 197 nucleotides, respectively). If the leading DNA polymerase stalls at the 5′ end of the *mat1*M cut template, it will produce a fragment of 196 nucleotides, migrating at the same position as the *mut1-4* fragment. Figure 6B shows that the leading-strand DNA intermediate co-migrates with the *mut1-4* size marker.

To validate the formation of a transitory blunt end, we performed ligation-mediated PCR (LM-PCR). The genomic DNA was ligated with phosphorylated, blunt-ended linkers. The ligation efficiency was analyzed by PCR, using nested PCR primers (1–2) to increase the specificity of the amplification and *mat1*-distal primers (3–4) as a control (Figure 6D).

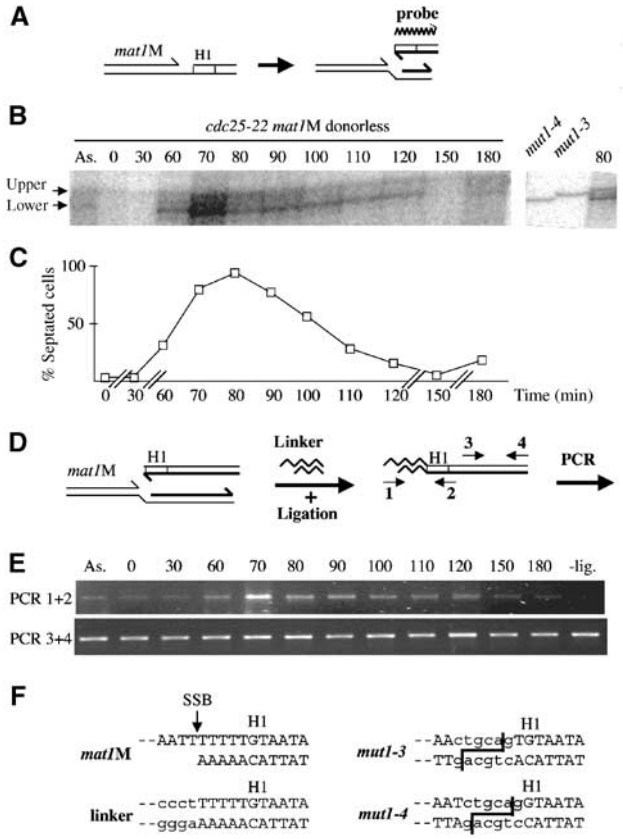

Figure 6 Mapping of the stalled leading-strand 3′ end at *mat1*. (**A**) Schematic representation of the stalled leading strand at *mat1* and polarity of the probe. (**B**) Autoradiogram of purified genomic DNA from a *cdc25-22 mat1*M donorless synchronized cell culture, digested with *Ssp*I and analyzed on a genomic sequencing gel. Left panel: Kinetics of the stalled leading strand. 'As.' represents the asynchronous cell population and the time (min) after release from the temperature block is indicated. The transitory band is labeled as 'lower' and the constant band as 'upper'. This upper band is due to low contamination of the labeled probe by the template used in the labeling reaction (data not shown). Right panel: Migration of the *mat1*M-distal lower strand of *mut1-3* and *mut1-4* digested by *Ssp*I and *Pst*I, together with the 80 min time point. The position of the *Pst*I sites are shown in (F), right panel. (**C**) Cell cycle progression was followed by measuring the proportion of septated cells (and cell density, not shown) as a function of time for almost two generations. Time is indicated in minutes (min). (**D**) Schematic representation of the LM-PCR method. Two pairs of primers were used: (1–2) and (3–4). (**E**) PCR products using primers (1–2) or (3–4) were amplified for 32 or 26 cycles, respectively, and analyzed on agarose gels. The time is indicated in minutes after temperature block and release. A '- lig' control experiment was also performed using the 70-min time point in the absence of ligase. (**F**) Sequence of the SSB in a *mat1*M donorless strain. The left panel shows the identical sequence obtained from eight independent clones of the LM-PCR products (using primers 1–2). An arrow indicates the position of the SSB and the linker sequence is written in lower-case letters. Right panel: *Pst*I sequences are indicated in lower-case letters and the cleavage sites are shown for *mut1-3* and *mut1-4* mutations.

As anticipated from the previous result, PCR products were observed from the DNA isolated during the DNA-replication period, concomitant with the presence of the stalled nascent leading strand (Figure 6E). The PCR product was cloned and sequenced. Figure 6F (left panel) shows the sequences of the amplified DNA, demonstrating the conserved and blunt-ended nature of the recombination intermediate.

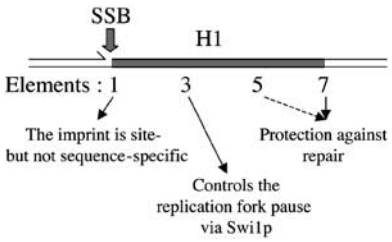

Figure 7 Role of the *cis*-acting elements in the H1 sequence. The positions of the SSB and the *cis*-acting elements are shown and their different roles in SSB formation and maintenance are indicated.

Discussion

Several novel *cis*-acting elements in the distal *mat1* sequence have been identified. These elements indicate that several molecular steps are required for efficient SSB formation and maintenance for mating-type switching (Figure 7).

SSB is site- but not sequence-specific

We found that our *Pst*I substitutions at the SSB site (*mut1*) did not change the position, or the efficiency of break formation, indicating distance-dependent and sequence-independent regulation of the SSB position. As compared to *mat1*M, the break at *mat1*P is shifted by three nucleotides (Nielsen and Egel, 1989), but the sequences to the right-hand side, containing H1, are identical for both *mat1*P and *mat1*M. Therefore, we should also reconsider the importance of sequence information within the P or M alleles. Future work is needed to understand how the position of the break is determined.

Replication fork progresses to the edge of the SSB 5′ end

Due to the presence of the *mat1*P DNA sequence in the initial DNA fragment used for homologous recombination, we propose that the removal of the *Pst*I mutation for *mut1* in the M allele is an obligatory step for initiating gene conversion. This proposal, together with leading-strand progression to the end of the break site, indicates that four heterologous nucleotides (within the *Pst*I sequence) are made upon strand invasion with the donor. These few bases might be removed soon after strand invasion by editing functions (polymerase or flap endonuclease activities), to allow priming of repair synthesis during gene conversion (Paques and Haber, 1997; Palmer *et al*, 2003). An additional argument for the 3′ end running to the edge of the SSB site comes from the (partial) persistence of the two distal *Pst*I substitutions (*mut2* and *mut3*) at *mat1*M upon switching. In these two mutants, only eight or 18 nucleotides within the 3′ end of the invading strand are perfectly homologous with the donor information. Removal of these heterologous sequences might require mismatch and/or excision repair factors, as shown in *S. cerevisiae* (Saparbaev *et al*, 1996; Sugawara *et al*, 1997). The efficient loss of the *Pst*I mutations, within a 20 bp window (*mut1–mut3*), followed a gradient, suggesting that the repair might be functionally linked to the initiation of DNA synthesis during gene conversion. This indicates that only 20 bp of perfect homology is needed for strand invasion at *mat1*.

To our knowledge, this is the first *in vivo* demonstration of a leading-strand polymerase reaching a DNA end. This is a recurrent question regarding telomere replication at native

ends of linear chromosomes. It is thought that leading-strand synthesis continues to the very end of the template molecule, but this was never formally demonstrated. The ability of the replication machinery to synthesize DNA to the very last nucleotide of a broken template seems a safe attempt to minimize the loss of DNA information. This raises important questions regarding how a replication fork (helicases or polymerases) senses and responds to oncoming damage. For example, is the entire replication fork maintained or collapsed before *mat1* switching? Is lagging and leading-strand synthesis transiently uncoupled, allowing the lagging-strand synthesis to proceed further, as recently proposed in *E. coli* (Pages and Fuchs, 2003)? Perhaps the novel *cis*-acting elements described here prevent the replication fork from collapsing, and/or assist in recruiting the homologous recombination machinery for gene conversion during mating-type switching.

Identification of the mat1 replication pause site

Previous work has shown that the *mat1* pause site 1 (*MPS1*) activity requires the function of both *swi1* and *swi3*, and might be one of the early steps in mating-type switching (Dalgaard and Klar, 2000). Significantly, we found that Swi1 interacts, directly or indirectly, with a short sequence present in H1 and that the *mut3* mutation almost abolishes this interaction. Furthermore, the mut3 site is necessary for *MPS1* function, whereas the two other elements defined by *mut5* and *mut7* play a minor role (Figure 4A). The pause acts upstream of the SSB formation, and protection or maintenance functions, revealed for the first time by *mut5* and *mut7*, act downstream of the SSB formation. Consequently, Swi1 is more likely involved in the formation and not protection of the SSB (see below). It was not possible to determine whether the mut3 site is sufficient for Swi1 function, since the protein is also required for the *mat1*-proximal replication-termination function (*RTS1*), consistent with the cumulative effect of iodine staining for the double-mutant strain *mut3* Δ*swi1* (data not shown). It is noteworthy that the modest Swi1 interaction observed with *RTS1* in the wild-type background seems stimulated in the *mut3*-containing strain. Previous observations indicated that the close proximity of *MPS1* and *RTS1* interferes with their functions (Dalgaard and Klar, 2001), but the role of *RTS1* was only described in an *Msmt*-0 mutant strain or on a plasmid, where SSB formation and switching are prevented. We imagine that the two replication fork barriers (RFBs), on either side of *mat1*, communicate with each other, such that Swi1 can interact with only one of the two sites, or that Swi1 interacts with both elements during the S-phase, but this interaction remains stable at *MPS1* and is only transitory during the S-phase at *RTS1*.

Finally, it was proposed that *RTS1* optimizes imprinting by controlling the direction of replication at *mat1* (Dalgaard and Klar, 2000). An additional function for *RTS1* might be to block any fork of replication running from the centromere-proximal side of *mat1*, especially during the mating-type switching process, which lasts about 30 min (at 24°C) and overlaps the replication period (Arcangioli and de Lahondes, 2000). This model is consistent with the proposed function of *S. cerevisiae* Tof1 (Swi1 in *S. pombe*) in the Mec1 (Rad3/ATR in *S. pombe*/humans) pathway, which is necessary to activate and maintain the S/M checkpoint (Foss, 2001). Recently, Tof1 was found to interact physically *in vivo*, with the replication machinery and stalled forks, using a global approach (Katou *et al*, 2003). Yet, we still do not know when and how Swi1 is recruited to the mut3 site in H1 and whether Swi1 is required to stop replication progression and/or to stabilize the stalled fork at *mat1*.

A model for chromosomal imprinting

A central question regarding programmed DNA rearrangements is how the recombination machinery is targeted to specific chromatin sites at the right time (Haber, 1998; Gellert, 2002). All of the double *cis*-acting mutant combinations tested exhibited a synergistic mating-type switching reduction, but never abolished switching, as observed by iodine staining (data not shown). This reinforces the idea that these *cis*-acting sites participate in concert for the initial process of mating-type switching. This feature is reminiscent of the ordered recruitment of transcription factors, allowing site-specific transcriptional initiation (Stargell and Struhl, 1996), in which some factors are able to first interact with DNA sequences in the presence of nucleosomes, thus permitting subsequent assembly of an enhanceosome (Merika and Thanos, 2001). The affinity of transcription regulators to specific DNA sequences is not sufficient, and only concerted binding leads to active enhanceosome assembly. To extend the previous imprinting model (Dalgaard and Klar, 2000), perhaps the Swi1-dependent replication fork pause allows Sap1 (de Lahondès *et al*, 2003) to interact with the SAS1 element, and this in turn facilitates further assembly of several, as yet, unidentified regulatory proteins to other *cis*-acting elements (mut5 and mut7 sites). This particular DNA–protein assembly might offer a multifunctional surface providing ordered, efficient and concerted DNA break formation on the neo-synthesized lagging strand, with the end result being that, during the S-phase, only one of the two sister chromatids is cleaved. Analysis of the chromatin nature at *mat1* will allow us to support this model. The apparent active protection of the SSB, revealed by the *mut7* mutation, suggested that the imprinting complex is a stable chromosomal structure of *mat1*, masking the SSB from repair. Consequently, during the subsequent DNA-replication period, two major events could be envisioned. The first event, associated with the leading-strand machinery, creates the blunt-ended DNA intermediate, channeling the homologous recombination machinery into mating-type switching. The second event, associated with the lagging-strand machinery, could reproduce the entire process of imprinting complex assembly, including SSB formation and its subsequent protection. This hypothetical scenario is proposed to explain the asymmetric pattern of mating-type switching in cell lineages of fission yeast. Finally, our results also raise interesting questions concerning how single-stranded lesions are maintained/protected and how repair occurs within different genomic regions/contexts.

The replication/recombination connection

The connection between replication fork progression and recombination is accumulating (Rothstein *et al*, 2000). It was traditionally proposed that both programmed and accidental pausing might lead to the formation of DSBs. The results described above suggest that DNA-replication fork pauses and single-strand DNA lesions are tightly associated.

Perhaps other programmed recombination events and systems possess a similar association. For example, DNA lesions have been detected in cell lines competent for somatic hypermutation or class switch recombination of immunoglobulin genes. These lesions are reported to be single stranded or double stranded, during the late S-phase (Papavasiliou and Schatz, 2000; Kong and Maizels, 2001; Haber, 2001). Another example is the RFB, found in the rDNA repeats of all eukaryotic organisms. In *S. cerevisiae*, the RFB has been associated with recombination hotspot activity and single-strand DNA lesions (Keil and Roeder, 1984; Brewer and Fangman, 1988; Weitao *et al*, 2003). Fragile chromosomal sites in higher eukaryotes are also induced by conditions that partially inhibit DNA replication. Furthermore, it was proposed that stalled replication forks, escaping the ATR replication checkpoint, induce common fragile-site expression (Casper *et al*, 2002), which may directly contribute to chromosome instability and tumor cell biology (Richards, 2001). Similarly, Mec1, the homolog of mammalian ATR in *S. cerevisiae*, prevents chromosomal breakage in replication-slow zones (Cha and Kleckner, 2002). Clearly, the progression of the replication fork along the DNA must translate the information required for chromosomal plasticity in a wide variety of biological systems.

Materials and methods

Strains

The *mat1*P DNA fragments containing the *Pst*I substitutions were introduced into the *mat1* locus by homologous recombination into the SP162 strain (*h90 leu1-32 ura4-D8*) using the lithium transformation procedure (Moreno *et al*, 1991), producing *mut1–mut10* mutant strains. Using the same procedure, the *mat1*M DNA fragments containing the *Pst*I substitutions were introduced by homologous recombination into the SP714 donorless strain (*mat1*M *leu1-32 ura4-D8 ade6-M210 mat2,3::LEU2*), producing strains *mut1-3* and *mut1-4*, respectively. Each construction has been sequenced.

A C-terminal HA tag of *swi1* within the chromosome was introduced using a PCR-based gene-targeting system (Bahler *et al*, 1998). The swi1-HA PCR product was transformed into either the *mat1*::*LEU2* derivative of SP837 (Arcangioli and Klar, 1991), producing strain AHR1, or *mut3*, producing strain AHR2. All primer sequences are available upon request.

Genomic DNA preparation and analysis

DNA was isolated by a classical method (Moreno *et al*, 1991), digested with the *Hind*III enzyme and analyzed by Southern blots. The probe was made using a 10.4 kbp *mat1*P *Hind*III fragment. Alternatively, DNA was prepared and digested (as indicated) in agarose plugs and resolved on an 8% denaturing PAGE (Arcangioli 1998). DNA was electroblotted on to a Hybond-N+ membrane (Amersham) for 1 h at 300 mA and revealed with a single-stranded probe immediately distal to H1. Single-stranded DNA probes, specific for the *mat1*-distal upper and lower strands, were prepared by primer extension and purified using denaturing PAGE conditions.

2D gels

2D gel analysis of replication intermediates was carried out as described previously (Brewer and Fangman, 1988). DNA was prepared and digested with *Nsi*I in agarose plugs (Arcangioli, 1998). Enriched fractions for replication intermediates were obtained using BND cellulose columns. Gels were hybridized with a 2.6 kbp *mat1*-distal specific fragment, containing *LEU2* from *S. cerevisiae*.

Synchronization conditions

Strains were grown in YES media, at 33°C, until exponential phase. Synchronization was achieved using lactose gradients, as described previously (Arcangioli, 2000), except that two consecutive lactose gradient centrifugations were performed. Small G2 cells (5% of the cells) from the initial culture were collected and incubated in prewarmed YES media at 33°C. The *cdc25-22* temperature-sensitive allele blocks the cell cycle at the G2/M transition at the nonpermissive temperature, allowing synchronous progression through the cell cycle, upon release at the permissive temperature. DNA was prepared and digested with restriction enzymes in agarose plugs. All synchronization experiments were performed at least twice.

ChrIP analysis

Exponential cultures of AHR1 (wt) and AHR2 (*mut3*) grown in YES at 33°C were crosslinked with formaldehyde for 12 min and sonicated such that the majority of sheared fragments were between 0.5 and 1.0 kbp. Whole-cell extraction, immunoprecipitation and DNA extraction of the immunoprecipitated material were performed as described (Meluh and Broach, 1999). The Anti-HA Affinity Matrix from Roche (anti-HA covalently bound to agarose beads) was used for the immunoprecipitation reactions. Samples were assayed by quantitative PCR with a LightCycler (ABI PRISM 7000 Sequence Detection System from Perkin-Elmer) according to the manufacturer's recommendations. Relative enrichments were obtained by first normalizing the total input DNA and ChrIP DNA to the furthest distal sequence, 5 kbp from the SSB, amplified by primer pair (i), as indicated in Figure 4B. The input normalized value was divided by the ChrIP normalized value, giving the full relative *in vivo* enrichment. ChrIP experiments were repeated at least twice, with independent DNA preparations. Primers for all PCR analyses were synthesized by GENSET SA guaranteed oligos, and chosen using the Primer Express™ Version 2.0 software (Perkin-Elmer). Primer pair sequences used for strain construction and ChrIP are available upon request.

Ligation-mediated PCR

The oligonucleotides BEL5A 5′OH TGACCTTTTGTAGGACAAGG TACCGGT TGTGAAGAAAGCCAATACCCT 3′OH and BEL5B 5′P AGGGTATTGGCTTTC 3′OH (Eurogentec) were hybridized, creating a blunt-ended linker for the LM-PCR reactions. DNA from the same time points obtained from the synchronized *cdc25-22* culture were prepared in agarose plugs, melted at 70°C for 10 min, and centrifuged. The supernatant was treated with RNAse (Roche) and β Agarase I (NEB). Genomic DNA at 5 ng/μl was mixed with the hybridized oligonucleotides at 0.2 μM and incubated with T4 DNA ligase and buffer (NEB) for at least 3 h at 16°C. The ligation product was directly used at a 1/20 dilution for 'Hot Start' PCR: 95°C (5 min), then 32 cycles at 94°C (30 s)/60°C (1 s)/72°C (30 s). The PCR product was digested and cloned into the pUC18 vector. Eight independent clones were sequenced and found to have identical, wild-type *mat1*M information.

Acknowledgements

We are grateful to G-F Richard and J Weitzman for reading the manuscript and contributing helpful comments. This work was supported by fellowships from the Ministère de l'Education National, de la Recherche et de la Technologie (MENRT) and La Ligue Contre le Cancer to AK, the European Molecular Biology Organization (EMBO) and the Fondation pour la Recherche Medical (FRM) to AH, as well as by grants from the Human Frontiers in Science Program (HFSP) and Association pour la Recherche sur le Cancer (ARC) to BA.

References

Arcangioli B (1998) A site- and strand-specific DNA break confers asymmetric switching potential in fission yeast. *EMBO J* **17:** 4503–4510

Arcangioli B (2000) Fate of mat1 DNA strands during mating-type switching in fission yeast. *EMBO Rep* **1:** 145–150

Arcangioli B, Copeland TD, Klar AJS (1994) Sap1, a protein that binds to sequences required for mating-type switching, is essential for viability in *Schizosaccharomyces pombe*. *Mol Cell Biol* **14:** 2058–2065

Arcangioli B, de Lahondes R (2000) Fission yeast switches mating-type by a replication-recombination coupled process. *EMBO J* **19:** 1389–1396

Arcangioli B, Klar AJS (1991) A novel switch-activating site (SAS1) and its cognate binding factor (Sap1) required for efficient *mat1* switching in *Schizosaccharomyces pombe*. *EMBO J* **10:** 3025–3032

Arcangioli B, Thon G (2003) Mating-types cassettes: structure, switching and silencing. In *Molecular Biology of Schizosaccharomyces pombe*, Egel R (ed), pp 129–147. Berlin: Springer Verlag

Bahler J, Wu J-Q, Longtine MS, Shah NG, McKenzie III A, Steever AB, Wach A, Philippsen P, Pringle JR (1998) Heterologous modules for efficient and versatile PCR-based gene targeting in *Schizosaccharomyces pombe*. *Yeast* **14:** 943–951

Beach DH (1983) Cell type switching by DNA transposition in fission yeast. *Nature* **305:** 682–688

Beach D, Nurse P, Egel R (1982) Molecular rearrangement of mating-type genes in fission yeast. *Nature* **296:** 682–683

Brewer BJ, Fangman WL (1988) A replication fork barrier at the 3′ end of yeast ribosomal RNA genes. *Cell* **55:** 637–643

Casper AM, Nghiem P, Arlt MF, Glover TW (2002) ATR regulates fragile site stability. *Cell* **111:** 779–789

Cha RS, Kleckner N (2002) ATR homolog Mec1 promotes fork progression, thus averting breaks in replication slow zones. *Science* **297:** 602–606

Crouse HV (1960) The controlling element in sex chromosome behavior in Sciara. *Genetics* **45:** 1429

Dalgaard JZ, Klar AJS (1999) Orientation of DNA replication establishes mating-type switching pattern in *S. pombe*. *Nature* **400:** 181–184

Dalgaard JZ, Klar AJS (2000) Swi1 and Swi3 perform imprinting, pausing and termination of DNA replication in *S. pombe*. *Cell* **102:** 745–751

Dalgaard JZ, Klar AJS (2001) A DNA replication-arrest site RTS1 regulates imprinting by determining the direction of replication at *mat1* in *S. pombe*. *Genes Dev* **15:** 2060–2068

de Lahondès R, Ribes V, Arcangioli B (2003) The fission yeast Sap1 protein is essential for chromosome stability. *Euk Cell* **2:** 910–921

Egel R, Beach DH, Klar AJS (1984) Genes required for initiation and resolution steps of mating-type switching in fission yeast. *Proc Natl Acad Sci USA* **81:** 3481–3485

Egel R, Eie B (1987) Cell lineage asymmetry in *Schizosaccharomyces pombe*: unilateral transmission of high-frequency state of mating-type switching in diploid pedigree. *Curr Genet* **12:** 429–433

Fantes PA, Nurse P (1978) Control of the timing of cell division in fission yeast. Cell size mutants reveal a second control pathway. *Exp Cell Res* **115:** 317–329

Foss EJ (2001) Tof1p regulates DNA damage responses during S phase in *Saccharomyces cerevisiae*. *Genetics* **157:** 567–577

Gellert M (2002) V(D)J recombination: RAG proteins, repair factors, and regulation. *Annu Rev Biochem* **71:** 101–132

Haber JE (1998) Mating-type gene switching in *Saccharomyces cerevisiae*. *Annu Rev Genet* **32:** 561–599

Haber JE (2001) Hypermutation: give us a break. *Nat Immunol* **2:** 902–903

Katou Y, Kanoh Y, Bando M, Noguchi H, Tanaka H, Ashikari T, Sugimoto K, Shirahige K (2003) S-phase checkpoint proteins Tof1 and Mrc1 form a stable replication-pausing complex. *Nature* **424:** 1078–1083

Keil RL, Roeder GS (1984) *Cis*-acting recombination-stimulating activity in a fragment of the ribosome DNA of *S. cerevisiae*. *Cell* **39:** 377–386

Kelly M, Burke J, Smith M, Klar A, Beach D (1988) Four mating-type genes control sexual differentiation in the fission yeast. *EMBO J* **7:** 1537–1547

Klar AJS (1987) Differential parental DNA strands confer developmental asymmetry on daughter cells in fission yeast. *Nature* **326:** 466–470

Klar AJS (1990) The developmental fate of fission yeast cells is determined by the pattern of inheritance of parental and grandparental DNA strands. *EMBO J* **9:** 1407–1415

Klar AJS, Miglio LM (1986) Initiation of meiotic recombination by double-strand DNA breaks in *Schizosaccharomyces pombe*. *Cell* **46:** 725–731

Kong Q, Maizels N (2001) DNA breaks in hypermutating immunoglobulin genes: evidence for a break-and-repair pathway of somatic hypermutation. *Genetics* **158:** 369–378

Meluh PB, Broach JR (1999) Immunological analysis of yeast chromatin. *Methods Enzymol* **304:** 414–430

Merika M, Thanos D (2001) Enhanceosomes. *Curr Opin Genet Dev* **2:** 205–208

Miyata H, Miyata M (1981) Mode of conjugation in homothallic cells of *Schizosaccharomyces pombe*. *J Gen Appl Microbiol* **27:** 365–369

Moreno S, Klar A, Nurse P (1991) Molecular genetic analysis of fission yeast *Schizosaccharomyces pombe*. *Methods Enzymol* **194:** 795–823

Nielsen O, Egel R (1989) Mapping of the double-strand breaks at the mating-type locus in fission yeast by genomic sequencing. *EMBO J* **8:** 269–276

Pages V, Fuchs RP (2003) Uncoupling of leading- and lagging-strand DNA replication during lesion bypass *in vivo*. *Science* **300:** 1300–1303

Palmer S, Schildkraut E, Lazarin R, Nguyen J, Nickoloff JA (2003) Gene conversion tracts in *Saccharomyces cerevisiae* can be extremely short and highly directional. *Nucleic Acids Res* **31:** 1164–1173

Papavasiliou FN, Schatz GG (2000) Cell-cycle-regulated DNA double-strand breaks in somatic hypermutation of immunoglobulin genes. *Nature* **80:** 216–221

Paques F, Haber JE (1997) Two pathways for removal of nonhomologous DNA ends during double-strand break repair in *Saccharomyces cerevisiae*. *Mol Cell Biol* **17:** 6765–6771

Park H, Sternglanz R (1999) Identification and characterization of the genes for two topoisomerase I-interacting proteins from *Saccharomyces cerevisiae*. *Yeast* **15:** 35–41

Richards R (2001) Fragile and unstable chromosomes in cancer: causes and consequences. *Trends Genet* **17:** 339–346

Rothstein R, Michel B, Gangloff S (2000) Replication fork pausing and recombination or 'gimme a break'. *Genes Dev* **14:** 1–10

Saparbaev M, Prakash L, Prakash S (1996) Requirement of mismatch repair genes *MSH2* and *MSH3* in the *RAD1–RAD10* pathway of mitotic recombination in *Saccharomyces cerevisiae*. *Genetics* **142:** 727–736

Singh J, Klar AJS (1993) DNA polymerase α is essential for mating-type switching in fission yeast. *Nature* **361:** 271–276

Stargell LA, Struhl K (1996) Mechanisms of transcriptional activation *in vivo*: two steps forward. *Trends Genet* **8:** 311–315

Styrkarsdottir U, Egel R, Nielsen O (1993) The *smt*-0 mutation which abolishes mating-type switching in fission yeast is a deletion. *Curr Genet* **23:** 184–186

Sugawara N, Pâques F, Colaiácovo M, Haber JE (1997) Role of *Saccharomyces cerevisiae* Msh2 and Msh3 repair proteins in double-strand break-induced recombination. *Proc Natl Acad Sci USA* **94:** 9214–9219

Weitao T, Budd M, Hoopes LL, Campbell JL (2003) Dna2 helicase/nuclease causes replicative fork stalling and double-strand breaks in the ribosomal DNA of *Saccharomyces cerevisiae*. *J Biol Chem* **278:** 22513–22522